Sparse nodes for velocity: Learnings from Atlantis OBN full-waveform inversion test

Jiawei Mei*, Zhigang Zhang, Feng Lin, Rongxin Huang, Ping Wang (CGG); Cheryl Mifflin (BHP)

Summary

As the key step in subsalt imaging, conventional salt model building has typically relied on manual interpretation of the salt geometry, which proves to be difficult for resolving complex salt models. As a result, subsalt imaging has been approaching a plateau in the last few years, largely because of our inability to improve the accuracy of salt models. Fast forward to today, where the recent success of using full-waveform inversion (FWI) to automatically update salt models and significantly improve subsalt images has opened the door to a new era of subsalt imaging. As FWI for salt model updates prefers data with good low frequencies, long offsets, and full azimuth, sparse nodes for velocity surveys were proposed to serve as an economic yet suitable acquisition solution for large-scale subsalt exploration. Because of FWI's prior inability to update salt models for field data, the feasibility of sparse nodes for velocity surveys was previously only studied on synthetic data, from which the conclusions might not be immediately applicable to field data. Using a recently-developed FWI algorithm that proves to work on salt in field data, and by decimating the densely-acquired Atlantis ocean bottom node (OBN) data, we studied the impact of sparse node data for FWI salt model updates. Based on the understanding gained from this, we further proposed and validated methods to improve FWI results with sparse nodes for velocity data.

Introduction

Subsalt imaging underwent a step change about fifteen years ago when the industry transitioned from narrow-azimuth (NAZ) data to wide-azimuth (WAZ) data (Threadgold et al., 2006; Michell et al., 2006) and from ray-based imaging algorithms, such as Kirchhoff and beam migration, to wave-equation-based imaging algorithms, such as reverse time migration (RTM) (Farmer et al., 2006; Zhang et al., 2007). Since then, incremental progress has been made in subsalt imaging with the availability of multi-WAZ or full-azimuth (FAZ) data (Moldoveanu and Kapoor, 2009; Mandroux et al., 2013) of increased illumination power, more accurate model formulations and derivations of sediment velocity (e.g., tilted traverse anisotropy or tilted orthorhombic anisotropy) (Zhang and Zhang, 2008; Han and Xu, 2012), and more advanced imaging algorithms (e.g., least-squares RTM) (Wong et al., 2011; Dai et al., 2013; Wang et al., 2016). However, salt model building, the key step for subsalt imaging, has remained dependent on manual interpretation of the salt geometry, which works well in areas with simple salt bodies but is very challenging in complex areas. The improvements to salt body images brought by FAZ data

with better illumination, better sediment models, and better imaging algorithms do help manual salt interpretation to some extent, but cannot solve the fundamental dilemma in manual salt model building – a good image of the salt body is required for a good salt model by manual interpretation, while a good salt model is required to provide a good image of the salt body in the first place. Other factors such as weak or diminished impedance contrast at the salt boundaries and dirty salt with variable velocities further hinder the manual salt model building process. For these reasons, manual salt model building has been the bottleneck for improvements in subsalt imaging, and even more so in recent years. The industry has recognized this issue and has been looking for better and more automatic salt model building methods for years, but with limited success. With recent breakthroughs in the algorithm, FWI has demonstrated the ability to automatically update salt models and bring a step change to subsalt images in some of the most complex areas (Shen et al., 2017; Michell et al., 2017; Zhang et al., 2018; Wang et al., 2019). With more demonstrated successes, automatic salt model building using FWI has opened the door to a new paradigm of subsalt imaging.

Successful FWI applications in salt environments and other complex geologic settings require data with good low frequencies to avoid cycle skipping, and long offsets and FAZ coverage to fully illuminate the target areas with diving waves. OBN data seems to be the natural choice because of the low ambient noise level at the ocean bottom and the stationary receiver patch that allows for recording long-offset and FAZ data more efficiently. However, it is still financially challenging to acquire OBN data for large-scale exploration purposes using the conventional layout of dense node and shot spacing. For this reason, sparse nodes for velocity surveys were recently proposed with the understanding that FWI for salt model updates can use much sparser data than required for imaging (Dellinger et al., 2017). Because of FWI's prior inability to update salt in field data, the feasibility of sparse nodes for velocity surveys was previously only studied on synthetic data, which often uses the same modeling engine to generate the target "field data" (an inverse crime) and cannot truly simulate the situation in a field data case (e.g., seismic amplitude mismatch between synthetic data and field data, random and coherent background noise). By using the recently-developed Time-Lag FWI algorithm (Zhang et al., 2018; Wang et al., 2019) that is proven to work on salt in field data, and by decimating the densely-acquired Atlantis OBN data, we simulated different scenarios of node and shot spacing to understand the key elements of sparse data for salt model updates and explored potential ways to

Sparse nodes for velocity

further improve FWI results with sparse nodes for velocity data.

Node and shot decimation testing

Since nodes and shots have different coverage, datum surfaces, and spacing/density in OBN case, the effects of node and shot decimation in FWI are not interchangeable. In order to understand the impact of node and shot spacing respectively, two sets of control tests were performed. In the first set of tests, the shot spacing of the FWI input was fixed at 100×100 m, while the node spacing increased gradually from 400×400 m to 2400×2400 m. As shown in

Figure 1, when the node spacing increased from 400×400 m to 2400×2400 m, the inverted model from 4 Hz FWI became noisier and overall the inversion converged more slowly, especially in complex areas, such as the cave marked by the white circles. However, the grand-scale images were comparable for node spacing ≤1200 m, which indicates the low wavenumber kinematic update is similar regardless of the noise level in the model. When node spacing further increased to 2400×2400 m, the image degraded appreciably compared to other scenarios with smaller node spacing, especially in the complex zone with low S/N, indicated by the blue circles.
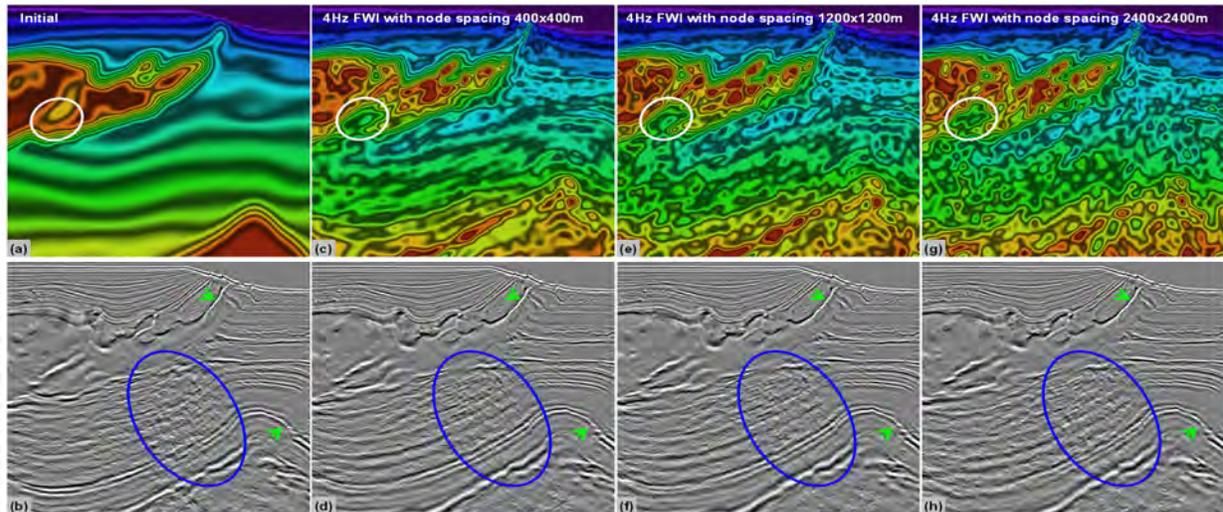

Figure 1: Node decimation test: 4 Hz FWI model with a fixed shot spacing of 100×100 m and the corresponding RTM image for different node spacing: (a)/(b) FWI initial model and the corresponding RTM image. (c)/(d) 400×400 m; (e)/(f) 1200×1200 m; and (g)/(h) 2400×2400 m. White circles mark the inverted cave in the model while blue circles indicate the low S/N region on the image. Green arrows indicate steeply dipping events.
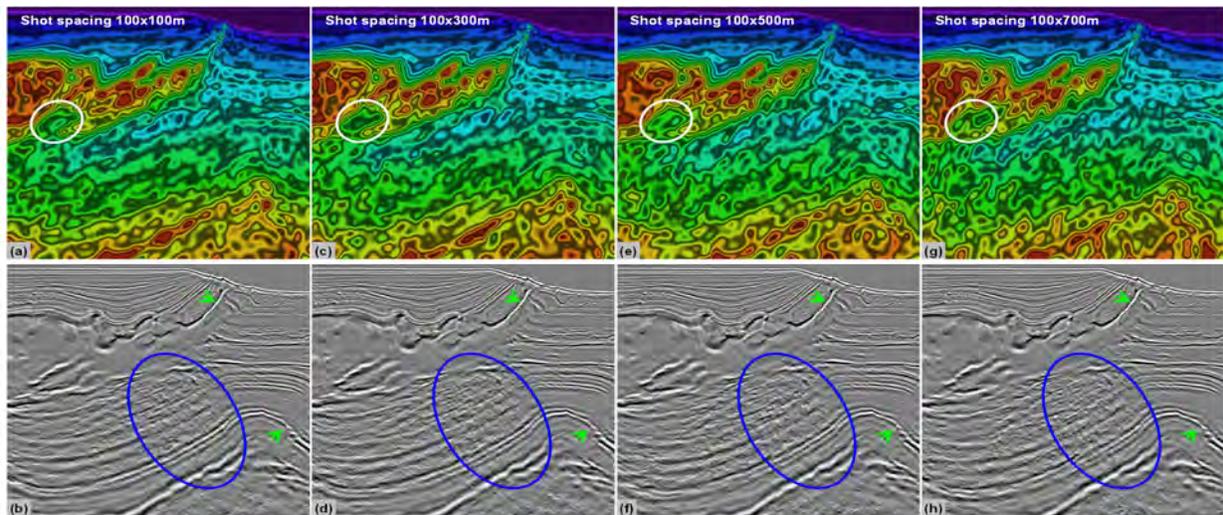

Figure 2: Shot decimation test: 4 Hz FWI model with a fixed node spacing of 1200×1200 m and the corresponding RTM image for different shot spacing: (a)/(b) 100×100 m; (c)/(d) 100×300 m; (e)/(f) 100×500 m; and (g)/(h) 100×700 m. White circles mark the inverted cave in the model while blue circles indicate the low S/N region on the image. Green arrows indicate steeply dipping events.

Similar to the node decimation testing, we performed the second set of control tests to understand the impact of shot spacing. We observed that, with a fixed node spacing of 1200×1200 m, the inverted models became increasingly noisier when the shot spacing increased from 100×100 m to 100×700 m. As a result, the migrated images deteriorated (Figure 2). The image degradation was most obvious in areas where the FWI models became very noisy.

From both sets of control tests, as node and/or shot sampling became increasingly sparse, the region that degraded first was the area with poor S/N, while the steeply dipping events, even the ones close to the water bottom, were well preserved. Does this mean the main culprit for the degradation of the model and image is the reduced S/N from the reduced total number of traces? Is spatial aliasing less of a problem? In the next section, we try to answer these questions with a synthetic study.

Spatial aliasing or S/N?

Mimicking the noise in field data and incorporating it into synthetic data is not a trivial process. However, we can exactly replicate the spatial sampling of the field data with synthetic modeling. The 11 Hz FWI model (Figure 3a) from non-decimated input was used as a "true" model to generate synthetic data. Two FWI tests using the same inversion scheme but different inputs, one with field data and the other with synthetic data (Figure 4), were performed. Both inputs were very sparse with a node spacing of 2400×2400 m and a shot spacing of 100×500 m. After running FWI up to 4 Hz, the inverted model (Figure 3c) from the sparse field data was very noisy and degraded the subsalt image (Figure 3d). Conversely, FWI using the synthetic data was able to recover the "true"
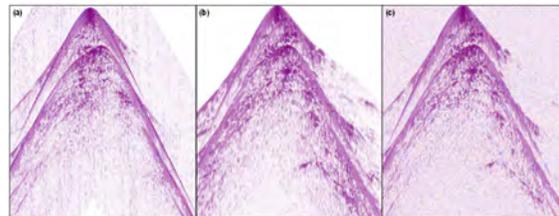

Figure 4: A sample node gather of one shot line for (a) field data; (b) synthetic data; and (c) synthetic data plus 20% random noise.

model almost perfectly (Figure 3e), and the corresponding RTM image was almost identical to the one from the "true" model. However, after adding random noise, which was 20% of the synthetic RMS amplitude, to the synthetic data (Figure 4c), FWI using this input failed to recover the true model. The inverted model was even noisier than in the field data case.

Though the pure synthetic case without added noise is an inverse crime, the conclusion on the impact of spatial sampling is still valid. The discrepancy between the field data case and the case of synthetic data without noise demonstrates that the degradation of the model and image from sparse field data is not due to spatial aliasing but mainly because of the reduced S/N from the reduced total number of traces. The result from synthetic data with random noise added further confirms the impact of reduced S/N. "Spatial aliasing" can be significant if it is severe, but in the normal range of node/shot spacing discussed here, the first order effect is S/N.

In addition, under such a sparse setting (2400×2400 m node spacing and 100×500 m shot spacing), the nearly-perfectly inverted model from FWI using synthetic input
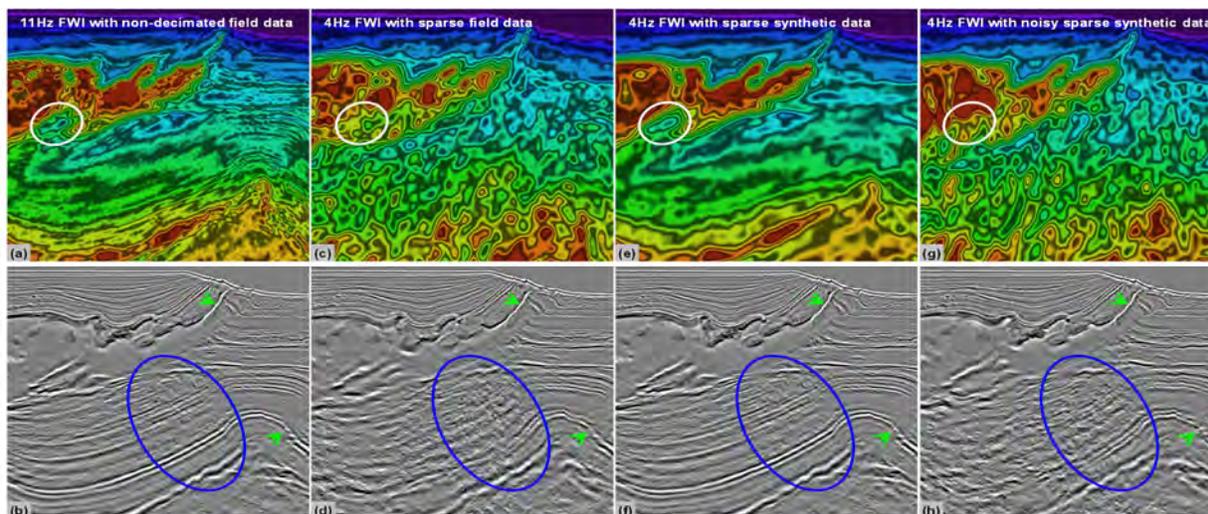

Figure 3: (a) is the "true" velocity model and (b) is the corresponding RTM image. 4 Hz FWI model with a node spacing of 2400×2400 m and a shot spacing of 100×500 m, and the corresponding RTM image using different input data: (c)/(d) field data; (e)/(f) synthetic data; and (g)/(h) synthetic data with 20% random noise. White circles mark the inverted cave in the model while blue circles indicate the low S/N region on the image. Green arrows indicate steeply dipping events.
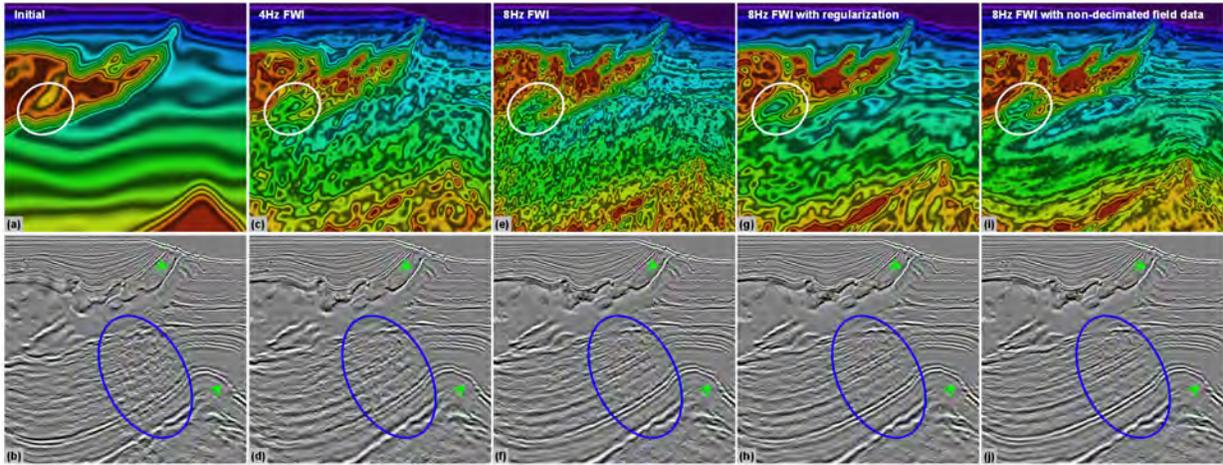
Figure 5: With a node spacing of 1200×1200 m and a shot spacing of 100×500 m, the velocity model and the corresponding RTM image for: (a)/(b) Initial model; (c)/(d) 4 Hz FWI model; (e)/(f) 8 Hz FWI model; (g)/(h) 8 Hz FWI model with regularization; and (i)/(j) 8 Hz FWI model with non-decimated input.

indicates that FWI is able to handle sparse spatial sampling in a way similar to least-squares migration.

How to further improve FWI results with sparse input?

From both the field data and synthetic studies, we learned that the impact of sparse node and shot spacing on FWI is mainly from the increased noise level in the inverted model due to the reduced S/N as a result of the sparse data. The next question we tried to answer is how to mitigate this effect and improve the FWI result. Our strategies were as follows:

- Run FWI to higher frequencies, because higher frequency data have higher S/N
- Apply regularization to suppress noise during inversion

Although the model from FWI using sparse input became noisier from 4 Hz to 8 Hz, as shown in Figure 5, the benefit of higher frequency inversion is clear on the image thanks to the improved S/N of higher frequency data and the increased resolution of the inverted salt model. Furthermore, a newly-developed regularization in FWI (Zhang, personal communication, 2019) was able to suppress the noise in the model, improve the model conformity, and preserve the salt velocity and salt boundary. This cleaner model led to a further improved image, especially in the low S/N area. However, the model and image are still not as good as those from FWI with non-decimated input. The difference indicates that accurate reservoir imaging in development fields may still require a node survey with dense node and shot spacing.

Discussion and conclusion

The decimation study using Atlantis OBN data confirms sparse nodes for velocity data can provide an economic yet effective solution for automatic model building using FWI in complex salt areas for exploration purposes. For a survey with the required offsets and node/shot coverage to adequately illuminate the target area with diving waves, an acquisition scheme with ~1000×1000 m node spacing and ~100×300 m shot spacing is deemed reasonable for FWI with sparse OBN data in deep-water regions. Further increase of maximum offsets and node/shot coverage can potentially relax the spacing requirements.

Spatial aliasing is not the bottleneck for FWI using sparse node data, as was shown in the synthetic study. Instead, noise – anything that we cannot replicate in the forward modeling during FWI, such as background noise, amplitude mismatch between field data and synthetic data, etc. – will manifest more severely on the results when using sparser data. The greatly improved results when running to higher frequency and applying regularization in FWI confirmed that the S/N of data plays the most crucial role in FWI using sparse nodes for velocity data.

Several approaches can be taken to further improve the FWI results with sparse nodes for velocity data. On the acquisition side, more powerful seismic sources, especially at the low frequency end, can be used to overcome the background noise and improve the S/N of data (Dellinger et al, 2016; Brenders et al., 2018). On the processing side, more advanced regularization schemes in both data and model domains can be developed to better suppress the noise in the inverted model; additionally, more accurate forward modeling in FWI with more realistic physics, e.g., anisotropy, absorption, and elasticity, will help in reducing the mismatch between synthetic and field data.

REFERENCES

Brenders, A., J. Dellinger, C. Kanu, Q. Li, and S. Michell, 2018, The Wolfspar® field trial: Results from a low-frequency seismic survey designed for FWI: 88th Annual International Meeting, SEG, Expanded Abstracts, 1083–1087, https://doi.org/10.1190/segam2018-2996201.1.

Dai, W., Y. Huang, and G. T. Schuster, 2013, Least-squares reverse time migration of marine data with frequency-selection encoding: Geophysics, **78**, no. 4, S233–S242, https://doi.org/10.1190/geo2013-0003.1.

Dellinger, J., A. J. Brenders, J. R. Sandschaper, C. Regone, J. Etgen, I. Ahmed, and K. J. Lee, 2017, The Garden Banks model experience: The Leading Edge, **36**, 251–158, https://doi.org/10.1190/tle36020151.1.

Dellinger, J., A. Ross, D. Meaux, A. Brenders, G. Gesoff, J. Etgen, J. Naranjo, G. Openshaw, and M. Harper, 2016, Wolfspar®, an FWI-friendly ultralow-frequency marine seismic source: 86th Annual International Meeting, SEG, Expanded Abstracts, 4891–4895, https://doi.org/10.1190/segam2016-13762702.1.

Farmer, P. A., I. F. Jones, H. Zhou, R. I. Bloor, and M. C. Goodwin, 2006, Application of reverse time migration to complex imaging problems: First Break, **24**, 64–73.

Han, W., and S. Xu, 2012, Raytracing and traveltime calculations for orthorhombic anisotropic media: 74th Annual International Conference and Exhibition, EAGE, Extended Abstracts, A023, https://doi.org/10.3997/2214-4609.20148363.

Mandroux, F., B. Ong, C. Ting, S. Mothi, T. Huang, and Y. Li, 2013, Broadband, long-offset, full-azimuth, staggered marine acquisition in the Gulf of Mexico: First Break, **31**, 125–132.

Michell, S., X. Shen, A. Brenders, J. Dellinger, I. Ahmed, and K. Fu, 2017, Automatic velocity model building with complex salt: Can computers finally do an interpreter's job?: 87th Annual International Meeting, SEG, Expanded Abstracts, 5250–5254, https://doi.org/10.1190/segam2017-17778443.1.

Michell, S., E. Shoshitaishvili, D. Chergotis, J. Sharp, and J. Etgen, 2006, Wide azimuth streamer imaging of Mad Dog; Have we solved the subsalt imaging problem?: 76th Annual International Meeting, SEG, Expanded Abstracts, 2905–2909, https://doi.org/10.1190/1.2370130.

Moldoveanu, N., and J. Kapoor, 2009, What is the next step after WAZ for exploration in the Gulf of Mexico?: 79th Annual International Meeting, SEG, Expanded Abstracts, 41–45, https://doi.org/10.1190/1.3255750.

Shen, X., I. Ahmed, A. Brenders, J. Dellinger, J. Etgen, and S. Michell, 2017, Salt model building at Atlantis with full waveform inversion: 87th Annual International Meeting, SEG, Expanded Abstracts, 1507–1511, https://doi.org/10.1190/segam2017-17738630.1.

Threadgold, I. M., K. Zembeck-England, P. G. Aas, P. M. Fontana, D. Hite, and W. E. Boone, 2006, Implementing a wide azimuth towed streamer field trial: The what, why and mostly how of WATS in Southern Green Canyon: 76th Annual International Meeting, SEG, Expanded Abstracts, 2901–2904, https://doi.org/10.1190/1.2370129.

Wang, P., A. Gomes, Z. Zhang, and M. Wang, 2016, Least-squares RTM: Reality and possibilities for subsalt imaging: 86th Annual International Meeting, SEG, Expanded Abstracts, 4204–4209, https://doi.org/10.1190/segam2016-13867926.1.

Wang, P., Z. Zhang, J. Mei, F. Lin, and R. Huang, 2019, Full-waveform inversion for salt: A coming of age: The Leading Edge, **38**, 304–213, https://doi.org/10.1190/tle38030204.1.

Wong, M., S. Ronen, and B. Biondi, 2011, Least-squares reverse-time migration/inversion for ocean bottom data: A case study: 81st Annual International Meeting, SEG, Expanded Abstracts, 2369–2373, https://doi.org/10.1190/1.3627684.

Zhang, H., and Y. Zhang, 2008, Reverse time migration in 3D heterogeneous TTI media: 78th Annual International Meeting, SEG, Expanded Abstracts, 2196–2200, https://doi.org/10.1190/1.3059322.

Zhang, Y., J. Sun, and S. Gray, 2007, Reverse-time migration: Amplitude and implementation issues: 77th Annual International Meeting, SEG, Expanded Abstracts, 2145–2149, https://doi.org/10.1190/1.2792912.

Zhang, Z., J. Mei, F. Lin, R. Huang, and P. Wang, 2018, Correcting for salt misinterpretation with full-waveform inversion: 88th Annual International Meeting, SEG, Expanded Abstracts, 1143–1147, https://doi.org/10.1190/segam2018-2997711.1.